



Improving the sensitivity of cellulose fiber-based lateral flow assay by incorporating a water-dissolvable polyvinyl alcohol dam

Nur Alam · Li Tong · Zhibin He · Ruihua Tang · Laboni Ahsan ·
Yonghao Ni

Received: 26 May 2021 / Accepted: 12 July 2021 / Published online: 17 July 2021
© The Author(s), under exclusive licence to Springer Nature B.V. 2021

Abstract Lateral flow assay (LFA) is an important point-of-care (POC) test platform due to the associated portability, on-site testing, and low cost for diagnosis of pathogen infections and disease biomarkers. However, compared to high-end analyzers in hospitals, LFA devices, in particular, paper-based LFA tests, fall short in accuracy. This study focuses on two ways to improve LFAs: (1) using cellulose fibers, rather than glass fibers for a sample pad, and (2) incorporating a one-step simple, facile, and low cost PVA dam into the LFA. Both strategies (cellulose fiber as a sample pad and water dissolvable PVA dam) contributed to delaying the controlled biomolecule's flow through

the nitrocellulose membrane's capillary channels resulting in increased bio-recognition time, thus contributing to the enhancement of LFA sensitivity. PVA modified cellulose fiber-based LFA demonstrated 10 times higher sensitivity than the cellulose fiber-based unmodified LFA, whereas 2 times enhancement was obtained in the cellulose fiber-based sample pad LFA compared to the glass fiber-based sample pad LFA. Ultimately, 20 times increase in sensitivity was achieved in the modified LFA device. This study shows that PVA and eco-friendly cellulose fibers could be incorporated into other paper based POC testing devices for future development.

Supplementary Information The online version contains supplementary material available at <https://doi.org/10.1007/s10570-021-04083-3>.

N. Alam · L. Tong · Z. He · R. Tang (✉) · Y. Ni (✉)
Department of Chemical Engineering, University of New
Brunswick, Fredericton, NB E3B 5A3, Canada
e-mail: tangruihua@163.com

Y. Ni
e-mail: yonghao@unb.ca

R. Tang
College of Bioresources Chemical and Materials
Engineering, Shaanxi University of Science &
Technology, Xi'an 710021, People's Republic of China

L. Ahsan
Labaid Ltd (Diagonestic and Reference Lab), Dhanmondi,
Dhaka, Bangladesh

Keywords Lateral flow assay (LFA) · Cellulose
fiber · Sensitivity enhancement · Bio-recognition ·
Biosensor · PVA dam

Introduction

Paper-based biosensors have received much attention in point-of-care (POC) tests due to their rapid, user- and eco-friendly, low-cost, light weight, and portability attributes (Vashist et al. 2015; Wood et al. 2019). Compared to time-consuming laboratory diagnostic tests, POC tests are advantageous due to the short time it takes to obtain results (Jani and Peter 2013). For rapid diagnosis, POC tests can cover a wide range of

infectious diseases detection including HIV/AIDS, malaria (Drain et al. 2014), and most recently even COVID-19 (Tang et al. 2021) as well as noncommunicable diseases such as cancers, metabolic diseases, cardiovascular diseases (CVD) (Vashist et al. 2015; Dincer et al. 2017). Furthermore, due to its abundance, easy fabrication and green technology, the use of paper for lateral flow assays (LFAs) POC test devices are becoming attractive. The paper-based LFAs could have wide applications in food safety detection, clinical diagnosis, and environmental monitoring sectors (Huang et al. 2016; Gong et al. 2017). Though various labelling particles like quantum dots, latex beads, magnetic nanoparticles, fluorophore silica nanoprobe (Zhao et al. 2018), and up-conversion nanoparticles can be used in LFA (He et al. 2021), the colloidal gold nanoparticle (AuNP) is the most commonly used platform as the bio-labelling agent in LFAs for its visual readout because it does not require any sophisticated instrument or skilled healthcare professionals (Chapman et al. 2015). The labelling agent plays a significant role in LFA sensitivity. Most of the visual readout results come as “yes” or “no”, whereas quantification and its sensitivity are challenging. Fortunately, some POC techniques are available for quantitative measurement that are paper-based and instrument-free (Li et al. 2020). It is highly desirable to enhance the sensitivity of LFA-based POC testing (Hwang et al. 2016; Chen et al. 2020).

In this context, much effort has been made to improve the sensitivity; including but not limited to dual AuNP conjugates (Choi et al. 2010), layer-by-layer self-assembled gold nanoparticles (Huang et al. 2019), nitrocellulose (NC) membrane modification with cellulose nanofibers (Tang et al. 2019), use of chitosan on NC membrane (Tang et al. 2020), PDMS-barrier (Choi et al. 2016), sponge as a shunt (Tang et al. 2017), and flow delayed by wax barrier (Sena-Torralba et al. 2020).

Controlling the flow rate is an easy and inexpensive method to enhance sensitivity. Some recent advances demonstrate that controlling the reagents transportation by using dissolvable barriers (Fu et al. 2010; Lutz et al. 2013), sugar bridges (Houghtaling et al. 2013), and printed wax pillars (Rivas et al. 2014) are effective in achieving high analytical sensitivity. Delaying the flow rate (Sena-Torralba et al. 2020) increases the bio-

recognition time which contributes to improved sensitivity.

The sample pad is an essential part of paper-based LFAs, typically glass fiber is used due to the fact that it is easy to handle, has good tensile strength, and no affinity towards proteins. The function of the sample pad is to control the release of sample and gold conjugate. Cellulose fiber is relatively inexpensive and environment friendly, and cellulose fiber-based sample pads have been used to absorb blocking agents, release agents, and pH and ionic strength modifiers (Posthuma-Trumpie et al. 2009; Sajid et al. 2015).

In the paper industry, hydrolyzed poly vinyl alcohol (PVA) is applied as a binder for paper surface treatment, and it can also be added at the papermaking wet-end (Fatehi et al. 2011). In hydrogel application, PVA, which is rich in hydroxyl groups, forms strong crosslinked networks (Yuan et al. 2019), and PVA based hydrogels have various applications, including strain sensors (He et al. 2020; Hu et al. 2021). In addition, for its dissolvable polymeric barrier attribute, PVA has been used to program/automate sequential reactions in LFA (Han et al. 2020).

In the present study, we aim to slow the flow rate to enhance the LFA sensitivity by incorporating cellulose fibers as the sample pad. Different from glass fibers, cellulose fibers are rich in hydroxyl groups that can have strong interactions with the sample, slowing down the sample flow. This controlled delayed sample flow gives more interaction time within the biomolecules and contributes to the enhanced sensitivity.

Furthermore, the hydrolyzed poly vinyl alcohol (PVA) dam has been introduced into the NC membrane before the test line zone. PVA has a gradual water-soluble advantage, which contributes to the slow release of the sample into the reaction pad. The hypothesis is that a water soluble PVA dam would delay the analyte flow rate, thus increasing the bio-recognition interaction time, and contributing to the enhanced sensitivity. More reaction time leads to increased sensitivity. PVA was used to create a dam by blocking the capillary channels/pores of the NC membrane. Over time it dissolves gradually and is allowed to pass through the target molecules along with labelling gold nanoparticles.

First, we studied the replacement of the glass fiber sample pad with a cellulose fiber sample pad. Then, the amount of PVA used was optimized, in terms of both the PVA concentration and the PVA volume.

Finally, a wide range of analyte concentrations were tested with both unmodified and PVA modified LFA devices for the comparative study.

Materials and methods

Materials and equipment

Bovine serum albumin, phosphate buffered saline (PBS), borate buffer, hydrogen tetrachloroaurate (III) trihydrate ($\text{HAuCl}_4 \cdot 3\text{H}_2\text{O}$, 99.9%), sodium citrate ($\text{Na}_3\text{C}_6\text{H}_5\text{O}_7 \cdot 2\text{H}_2\text{O}$), human IgG (hIgG) from human serum (I2511), anti-human IgG (I1886), anti-human IgG (γ -chain specific)-biotin (B1140), and hydrolyzed poly vinyl alcohol (PVA, $M_w = 31,000\text{--}50,000$; 98–99% hydrolyzed) were purchased from Sigma-Aldrich (USA). Rabbit anti-goat IgG (305,006,003) was purchased from Jackson Immunoresearch Lab (USA). NC membrane (HF120) was obtained from Millipore Sigma (USA), while the sample pad, absorbent pad, and conjugate pad were purchased from Shanghai Kinbio Tech Co., Ltd (China). All chemical reagents were analytical grade.

Refrigerated centrifuge Allegra X-30R (Beckman Coulter, USA) was used to separate conjugated gold nanoparticle; evolution 201 UV–visible spectrophotometer (thermo scientific) was used to optimize gold conjugation; automated lateral flow reagent dispenser (ALFRD) fusion 200 syringe (ClaremontBio, USA) was used to dispense control and test line on NC membrane; an automated cutter (ZQ2002, Kinbio Tech. Co., Ltd, China) was used to cut assembled card into device/strips; ESEQuant LR3 Gold strip reader (QIAGEN, Germany) was used to read strips into signal for the quantitative analysis. Transmission electron microscopy (TEM) images were obtained by a JEOL 2011 (Japan) with a 200 kV acceleration voltage, while scanning electron microscopy (SEM) results were obtained using a JEOL JSM6400 (Japan). Porosity measurement was performed by using Tele-dyne Gurley (USA).

Preparation of gold nanoparticles (AuNPs)

Colloidal gold nanoparticle was prepared by adding 0.01% HAuCl_4 and stabilized with 0.024% sodium citrate in a 1L round-bottom flask, and the mixture was boiled until it became the color of red wine (Khan et al.

2016). The colloidal gold was then filtered through a 0.2 μm syringe filter. The average size of AuNPs is 27 nm, which was determined based on TEM images and image analysis using ImageJ software. The as-prepared AuNPs were stored in a dark bottle at 4 °C. All glassware was cleaned with *aqua regia* overnight and rinsed with deionized water.

Bio-labelling of AuNPs

The AuNPs modification followed a procedure reported in the literature (Rivas et al. 2014). In brief, the pH of the AuNP suspension was adjusted to 9.15 with borate buffer (0.1 M); following that, a 100 μL of 100 $\mu\text{g mL}^{-1}$ anti-human IgG (γ -chain specific)-biotin aqueous solution was added to 1.5 mL of the AuNP suspension. This solution was incubated for 20 min and shaken at 400 rpm. Then, 100 μL of 1 mg mL^{-1} BSA aqueous solution was added and shaken for another 20 min at 400 rpm. To separate the conjugated gold nanoparticles, the suspension was centrifuged at 14,000 rpm and 4 °C for 25 min. The supernatant was removed gently and the pellet of AuNP/anti-human IgG was resuspended with 500 μL of borate buffer containing 10% sucrose (2 mM, pH 7.4). The glass fiber gold conjugate pad was dipped into it, and vacuum dried for 1 h (hour).

Preparation of PVA concentration in solution

A homogeneous aqueous PVA solution was prepared by dissolving it in deionized water. First, sonication of 2 h at 60 °C; then shaken for 2 h at 400 rpm and 25 °C. Finally, vacuum degassing for 30 min at 25 °C.

LFAs preparation

Sample pads were treated by dipping into 10 mM PBS (pH 7.4), 5% BSA and 0.05% Tween[®]-20, and drying at 60 °C for 2 h. Antibodies for test (capture, anti-human IgG) and control (Rabbit anti-goat IgG) lines were prepared as 1 mg mL^{-1} to dispense onto nitrocellulose membrane with ALFRD dispenser (2.0 $\mu\text{L cm}^{-1}$). Then, the sample pad, gold conjugate pad, nitrocellulose membrane, and absorbent pad were assembled sequentially overlapping each other by 2 mm. The assembled card was cut to 4.0 mm wide to prepare LFA strips. Finally, PVA solutions were placed as a drop between the gold conjugate pad and

test line to create a dam. These LFAs were dried for 1 h at 37 °C before use. It is noted that, the PVA dam was not used in glass fiber-based sample pad LFA device.

Porosity and flow rate determination assay

Porosity measurement was performed by air resistance (Gurley method). It is quantified by obtaining the time for a given volume of air flow through a specimen of given dimension under a specified pressure, pressure difference, temperature, and relative humidity (TAPPI test method, T 460 om-96). In addition to porosity, the sample flow rate was calculated by video analysis.

Optimization assay

Under the same conditions, the treated glass fiber and cellulose fiber-based sample pad LFA devices were fabricated, and the sample flow rate was measured (only PBS was used). Both types of LFA devices were then tested with a wide range of sample concentrations (0–5000 ng mL⁻¹).

In terms of PVA optimization for cellulose fiber-based sample pad LFA, different concentrations of PVA dam (0–7.5% PVA) were prepared to obtain higher sensitivity. In this case, 2.0 µL PVA was used. Then, dams of different volumes (0–2.0 µL) of optimized concentration were applied with a 0.5 µL increment to study the volume effect. For every case, the flow rate was measured.

Samples flowed for 15 min and readings were taken with a strip reader immediately after 15 min. PBS without analyte was considered as blank. The blank had a background noise during the strip reader reading (though it was not visible to the naked eyes), and we made correction for the background noise for other samples. All the measurements were performed in triplicate.

Human IgG detection

Finally, the optimized LFA device was tested against sample solutions (human IgG) of different concentrations ranging from 0 to 2500 ng mL⁻¹ in PBS (10 mM, pH: 7.4) and 100 µL was dispensed on each strip. Sample run time was kept the same and readings were taken with a strip reader immediately after run completion.

Results and discussion

Concept of using PVA dam to enhance the sensitivity of cellulose fiber-based LFA

The sample flow rate has a strong effect on the sensitivity (Sena-Torralba et al. 2020). Effective strategies to slow down the flow rate can enhance the sensitivity of LFA devices (Rivas et al. 2014; Sena-Torralba et al. 2020). The lowered diffusion will allow longer reaction times with the reagents during the passing of target analyte over capture reagent through reaction membranes. As shown in Fig. 1, the NC membrane is working as the stationary phase, and the target analyte is the mobile phase. The slower passing of the mobile phase leads to more complete reactions to form bio-recognition between the analyte/AuNP-labelled antibody, which will bind with the test and control line biomolecules.

In the present study, we designed a PVA dam for slowing down the flow rate. Moreover, the use of a cellulose fiber-based sample pad, instead of a glass fiber-based sample pad slowed down the sample flow. PVA ($M_w = 31,000\text{--}50,000$; 98–99% hydrolyzed) is a water-soluble polymer. Initially, the PVA impregnation plugs the NC membrane pores, then as the analyte passes through, PVA gradually dissolves; such a process leads to the increased reaction time between the analyte and the AuNP-labelled antibody, responsible for the increased sensitivity. The concept is schematically illustrated in Fig. 1, both the unmodified and PVA modified LFA devices are included for comparison (in both cases, cellulose fiber sample pad). The unmodified LFA device consists of a cellulose fiber sample pad, gold conjugate pad, NC membrane and an absorbent pad (Fig. 1A). For the PVA modified LFA device, the PVA dam is placed between the gold conjugate pad and the test line (Fig. 1B). In this case, the PVA dam effectively slows down the analyte flow, and the difference in the sample flow rate between the unmodified and modified device, is shown on the right side of the schematic diagram.

In Fig. 1C, a LED strip reader is used to quantify the signal intensity that is correlated to the target analyte. A larger peak indicates higher amounts of bio-recognition in the test and control line.

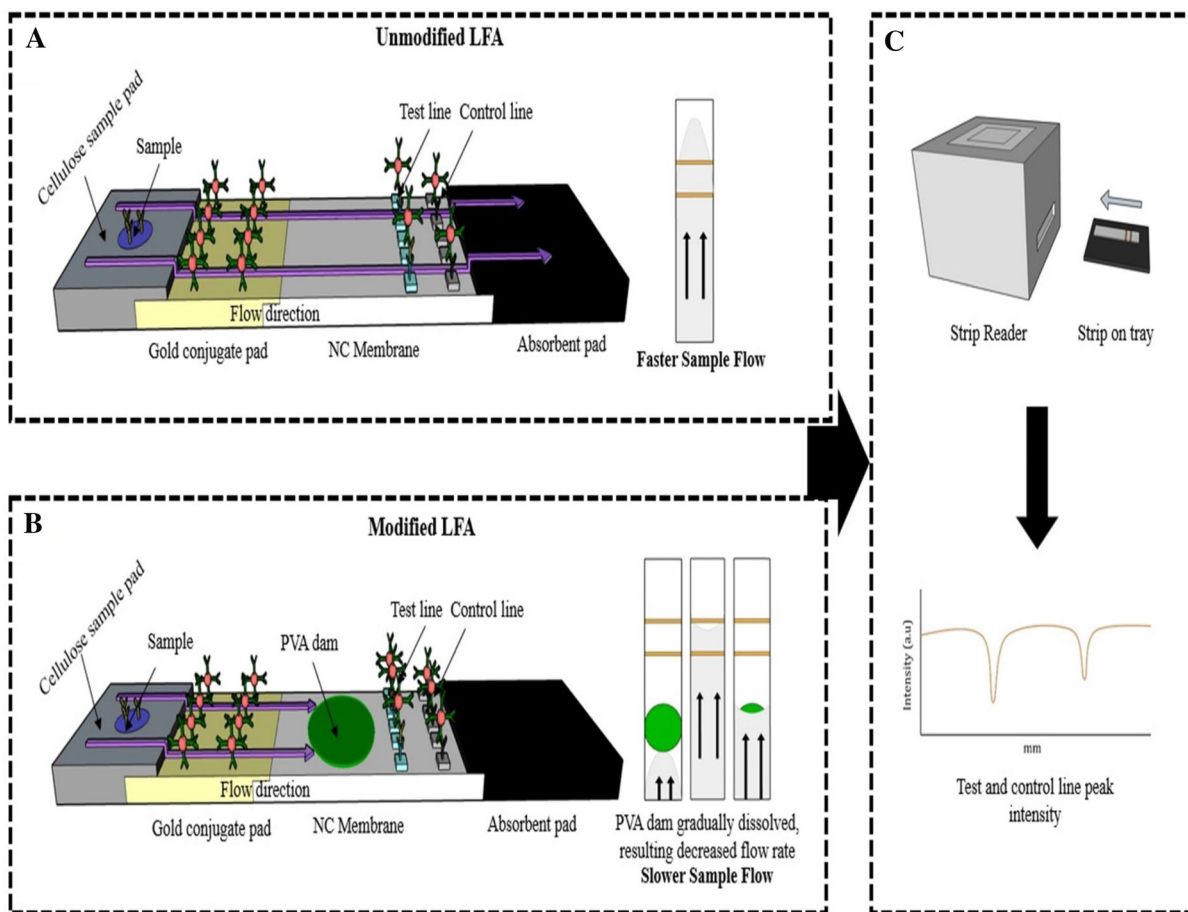


Fig. 1 Schematic of unmodified (A), and modified LFA (B) and strip reader for quantification (C). For the unmodified LFA device (A), it takes less time to pass through the reaction membrane (NC membrane). For the water-soluble polyvinyl

alcohol (PVA) dam modified LFA device (B), the flow delays significantly due to the presence of PVA dam (right side), resulting in enhanced sensitivity. A larger peak (C) relates to more analyte for quantification analysis by strip/device reader

Cellulose fiber-based sample pad versus glass fiber-based sample pad

In the present study, we used a cellulose fiber sample pad, and the results are compared with those using a glass fiber sample pad, which has been used in most of the publications in the literature. Cellulose fiber pad has a number of advantages: (1) the cellulose fiber pad has a lower porosity than the glass fiber pad, which was verified by the porosity measurements in accordance with the Gurley method (0.82 s for the cellulose fiber pad, and only 0.1 s for the glass fiber pad), (2) cellulose fibers have abundant hydroxyl groups that can interact with water (Fig. S1), both of which can lead to slowing down the analyte passing through the pad. In an early study by Chami Khazraji and Robert

(Chami Khazraji and Robert 2013), the immediate formation of a hydrogen bonding network was confirmed between cellobiose and water molecules.

As shown in Fig. S2, the results of flow rate are indirectly demonstrated by the differences in the time taken for PBS to flow through the 20 mm NC membrane between the glass fiber and cellulose fiber-based sample pad LFA, it takes 33s for PBS to migrate through the 20 mm NC membrane for the glass fiber-based sample pad device, which compares to 42s for the cellulose fiber sample pad under otherwise the same conditions. Again the differences in the pad porosity and functional groups in glass fiber and cellulose fiber, are responsible for these results.

The corresponding limit of detection (LOD) for glass fiber-based device and cellulose fiber-based

device was 1000 ng mL^{-1} , 500 ng mL^{-1} , respectively (Fig. S3). Therefore, we conclude that in comparison with the glass fiber-based sample pad, the cellulose fiber-based sample pad enhances the sensitivity 2 times. In the remaining study, we used the cellulose fiber-based sample pad LFA device.

Effect of PVA concentration

NC membrane was treated with different concentrations of PVA. The resultant NC membrane's porosity, sensitivity and flow rate are illustrated in Fig. 2. Pores of NC membrane are blocked by the PVA treatment and a higher PVA concentration leads to more effective blockage (Fig. 2A). For the control sample (no PVA), pores are distinctly visible (Fig. 2A(a)). SEM images clearly indicate that as the PVA concentration increases during the treatment (2.0 μL applied in each of these cases), more blockages become evident.

We also determined the pore size of these samples by using ImageJ software. For the control, it is $17 \pm 1 \mu\text{m}$; while it is $15 \pm 5 \mu\text{m}$, $10 \pm 3 \mu\text{m}$ and $6.0 \pm 2 \mu\text{m}$ for the samples' treatment with 2.5%, 5.0%, and 7.5% PVA, respectively. These pore size results are in agreement with the SEM results.

We then determined the sensitivity of the LFA device treated with different PVA concentrations, using human IgG as analyte, which is in a range of 0–500 ng mL^{-1} . Naked eye observation (Fig. 2B(a)) indicates that the sensitivity improves as a result of the PVA treatment, which increases as the PVA concentration increases. With a 7.5% PVA concentration, LOD is 50 ng mL^{-1} . These results are consistent with the quantifying analysis from the strip reader (Fig. 2B(b)), showing that the 7.5% PVA-treated device gives the highest signal in all tests. The enhanced sensitivity from the PVA treatment is attributed to the decreased flow rate of the analyte.

The effect of different PVA concentrations on the flow rate is shown in Fig. 2C. For the devices treated with 2.5%, 5.0%, and 7.5% PVA, images were captured with the sample (PBS only) migrating at different times: 15s, 30s and 45s (seconds) (Fig. 2C(a)). Evidently, PVA slows down the flow rate: the higher the PVA concentration, the slower the flow rate. Flow pattern of the unmodified device (no PVA) is shown in Supporting Information (Fig. S2),

indicating a very fast process: only 42s to completely migrate through the whole NC membrane (20 mm).

Shown in Fig. 2C(b) is the migrating time versus distance at various PVA concentrations. For the same 20 mm NC membrane, the migrating times of the 0%, 2.5%, 5.0% and 7.5% PVA-treated samples, are 42, 54, 76, and 90s, respectively, confirming that a higher PVA concentration leads to a slower analyte flow rate.

Trials at higher than 7.5% PVA concentration were also conducted (Fig. S4), however, the results show that the signal intensity decreases, indicating that 7.5% PVA is the optimum concentration. It may be possible that excessive amounts of PVA molecules could compete with analyte for the reactions in the test line, decreasing the signal intensity and reaction is too slow to meet all analyte to reaction zone.

Effect of PVA volume

With the PVA concentration fixed at 7.5%, we studied the effect of different volumes of PVA solution, ranging from 0.5 to 2.0 μL , with 0.5 μL increment. The results show that in the range of 0.5–1.5 μL , a higher volume improves the sensitivity (Fig. 3A), while no further improvement in the sensitivity was observed when further increasing from 1.5 to 2.0 μL (Fig. 3A(b)). The device images (Fig. 3A(a)) also show that the best condition giving the highest sensitivity against the various sample concentrations (hIgG) is 1.5 μL of 7.5% PVA. Under such a condition, the visual observation indicates the LOD of hIgG is 50 ng mL^{-1} . In Fig. 3A(b), quantitative analysis also supported the visual results indicating that a higher volume improves the sensitivity. In our study, for the 4.0 mm width LFA device, 1.5 μL PVA was used, and it occupied the entire width of the 4.0 mm dam (Fig. S5).

We further studied the effects of different PVA volumes (0, 0.5, 1.0, 1.5, 2.0 μL) on the flow rate (Fig. 3B). In Fig. 3B(a), the sample flow migration patterns were recorded at the same time of 35s, showing that as the PVA volume increases (0, 0.5, 1.0, 1.5, 2.0 μL), the migration distance becomes less, indicating a slower flow rate. Furthermore, the migration time at various PVA volumes through the NC membrane is shown in Fig. 3B(b), it is evident that a higher PVA volume yields a longer time at the same distance; for completing the entire 20 mm NC

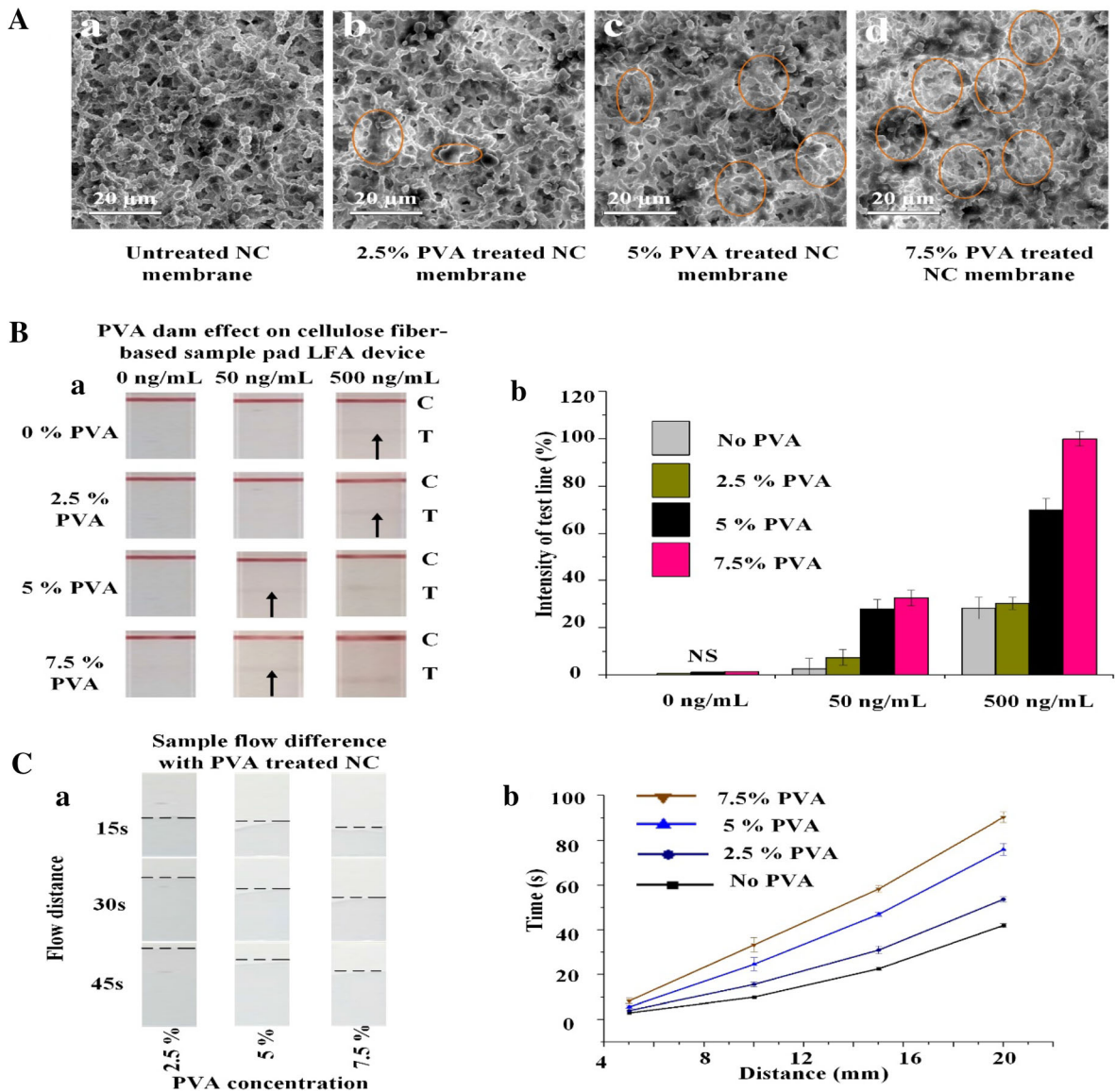


Fig. 2 Evaluation of PVA concentration effect on porosity, sensitivity, and flow rate. **A** SEM micrographs analysis: a higher PVA concentration on NC membrane leads to the decreased pore size ($17 \pm 1 \mu\text{m}$, $15 \pm 5 \mu\text{m}$, $10 \pm 3 \mu\text{m}$, $6.0 \pm 2 \mu\text{m}$ for untreated, 2.5%, 5.0%, 7.5% PVA-treated, respectively), with more pores blockage from (a) control (no block) to (d) 7.5% PVA (the marked circles indicates the blockage). **B** Sensitivity analysis: B(a) Qualitative analysis of various concentrations of

membrane, the calculated time is 42, 50, 56, 82, and 90s for 0, 0.5, 1.0, 1.5, and 2.0 μL PVA dam modified device, respectively.

PVA dam (2.0 μL) modified LFA device; B(b) Quantitative analysis of test line A higher PVA concentration dam shows a higher signal. **C** Flow rate analysis: C(a) Photographs of flow distance on NC membrane over time at various PVA concentrations (black dot line indicates the highest sample migration distance at certain time); C(b) Sample migration time versus distance at various PVA concentrations (T = test line and C = control line; NS indicates error bar is not significant)

Human IgG LOD determination

Based on the above results, we chose the optimum PVA concentration of 7.5% and PVA volume of 1.5 μL for the 4.0 mm width device for LOD determination. A comprehensive comparative study was carried

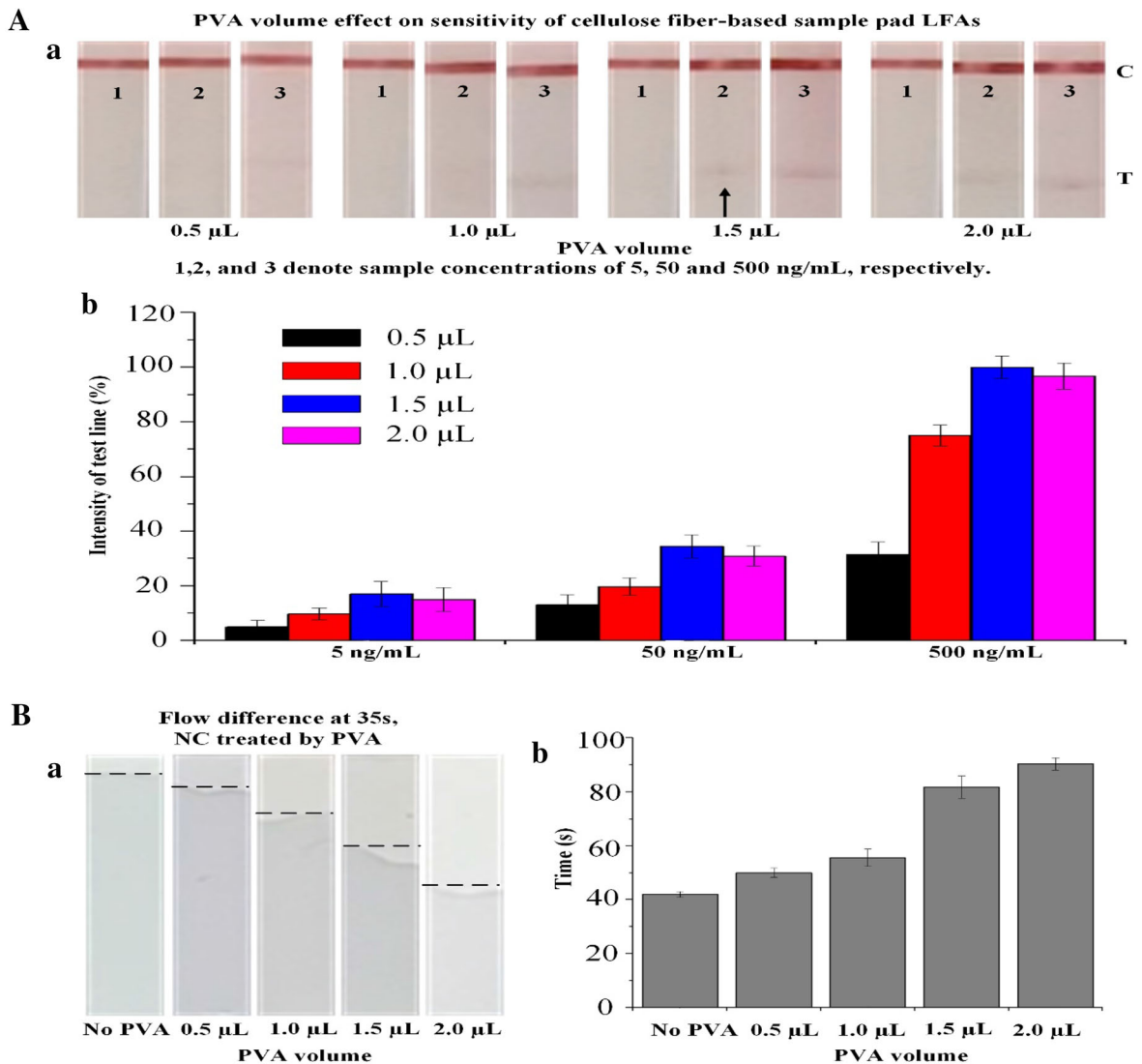


Fig. 3 Evaluation of 7.5% PVA volume effect on sensitivity, and flow rate. **A** Sensitivity analysis; A(a) Qualitative strip images at various sample concentrations (5, 50, and 500 ng mL⁻¹) with different PVA volumes (0.5, 1.0, 1.5, and 2.0 μL); A(b) Quantitative evaluation of the assay performed.

out for two devices: (1) the unmodified LFA, that is without PVA modification (W/O PVA), (2) PVA modified (7.5% PVA concentration, 1.5 μL PVA volume) LFA (Fig. 4).

As shown in Fig. 4A(a), the LOD of the unmodified (W/O PVA) is 500 ng mL⁻¹, and that for the PVA modified device is 50 ng mL⁻¹ (Fig. 4A(b)), indicating that the LOD increases 10 times as a result of PVA modification. The quantitative results from a wide range of sample concentrations, 0, 5, 50, 500, 1000,

B Flow rate evaluation on volume; B(a) PVA volume affects flow rate, flow distance at 35s (seconds). Black dot lines marked the maximum flow distance; B(b) time taken to migrate 20 mm NC membrane of different PVA volumes. (T = test line and C = control line)

and 2500 ng mL⁻¹, show that there is consistent improved signal intensity for the PVA modified device compared to the unmodified device.

The PVA dam effectively slows down the analyte flow through the LFA device with addition of a cellulose fiber sample pad; thanks to the highly soluble PVA and cellulose fiber sample pad, as the analyte passing through it, PVA gradually dissolves so that the analyte flow rate also gradually increases. Upon completion of the analysis, the SEM image of the

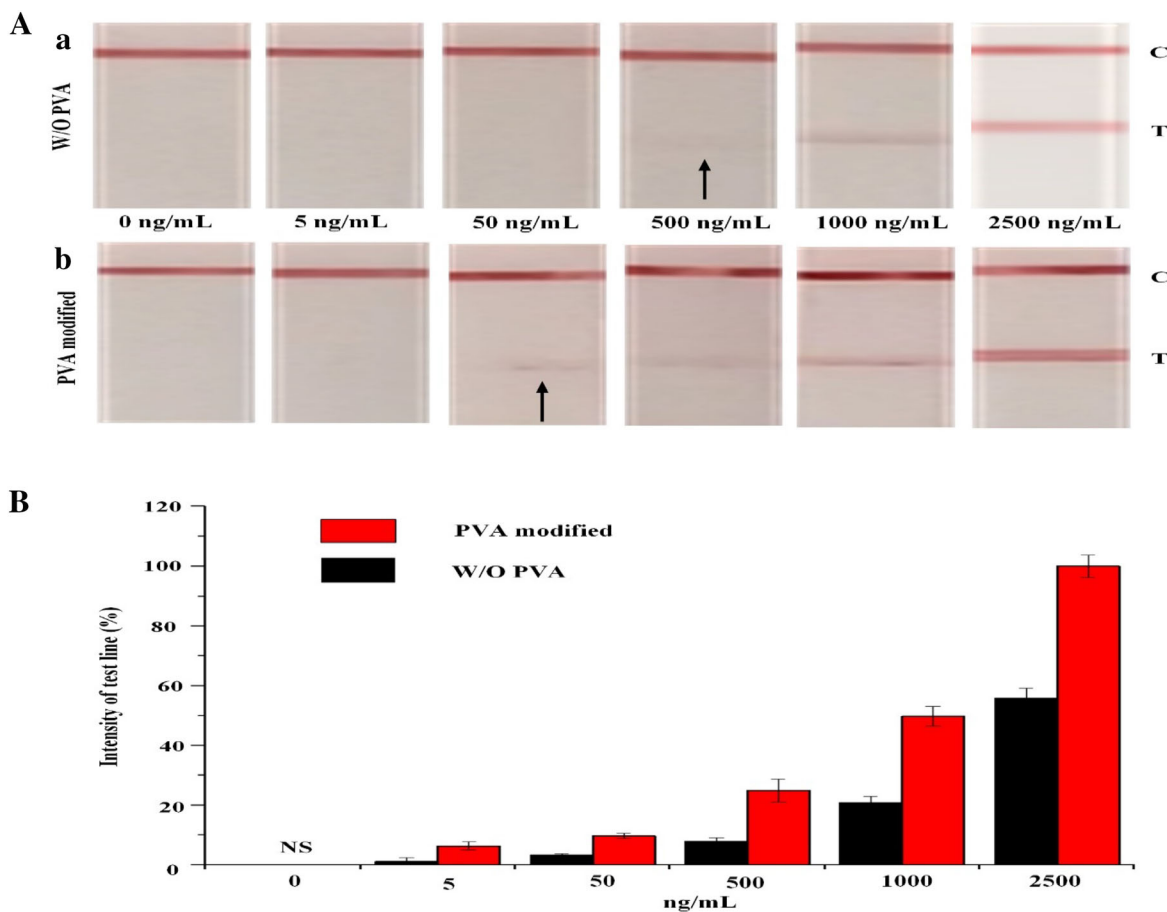


Fig. 4 Human IgG LOD evaluation. **A** Photographs of LFA devices; (a) Without PVA (W/O) or unmodified; and (b) PVA modified (7.5%, and 1.5 μL) devices against wide range human IgG (hIgG) concentrations. **B** Quantitative measurement of test

line for different sample concentrations (hIgG). The modified device has a LOD of 50 ng mL^{-1} , whereas unmodified device has a LOD of 500 ng mL^{-1} . (T = test line and C = control line; NS indicates error bar is not significant)

NC membrane (Fig. S6) proves that PVA is absent, indicating that PVA is totally dissolved and washed out in the process.

The concept of using a water-soluble PVA dam to increase sensitivity can be readily integrated into LFA for future development. The inclusion of the PVA dam allows more interaction time between the analyte and AuNp conjugate and finally with bio-recognizing molecules, the bioreceptor-based reactions, which may include antigen–antibody or nucleic-acids. In addition, this approach could also be applied to other modified LFAs with printed pillar design used as delaying microfluidics flow (Rivas et al. 2014), printed barriers (Choi et al. 2016), and inkjet-printing technology using a hydrophobic solution or an ink capable of well-defined patterns (Apilux et al. 2012) in

different regions of the membrane device to get more sensitive results.

Conclusion

In summary, this study demonstrates a simple strategy by incorporating a PVA dam into the NC membrane before the test line zone to significantly enhance the sensitivity of paper-based LFA devices. The results show that the analytical sensitivity improves from 500 to 50 ng mL^{-1} (10-fold higher) on the cellulose fiber-based sample pad LFA under the conditions of 7.5% and 1.5 μL PVA dam. The underlying mechanism is that the PVA dam delays the sample flow, thus increasing the bioreaction time and also improves the

sensitivity. In addition to this major improvement in our study, the use of a cellulose fiber sample pad instead of glass fiber increases the sensitivity by 2-fold.

This device is easy to fabricate, low-cost, not time-consuming and does not require additional lab set up for test and result interpretation. This modified paper-based LFA device can be readily incorporated into point-of-care and environment monitoring LFA platform; furthermore, the present study expands the application of eco-friendly cellulose material in point-of-care testing devices.

Acknowledgments This work was supported by the Canada Research Chairs Program of the Government of Canada (CRC 950231308), National Natural Science Foundation of China (21808132), China Postdoctoral Science Foundation (2018M633525), and the Chinese Scholarship Council (201908610073).

Declarations

Conflict of interest All authors declare that they have no conflict of interest.

Ethical approval The study was completed by following ethical standards; no animal or human participants were involved in the study.

References

- Apilux A, Ukita Y, Chikae M, Chailapakul O, Takamura Y (2012) Development of automated paper-based devices for sequential multistep sandwich enzyme-linked immunosorbent assays using inkjet printing. *Lab Chip* 13:126–135. <https://doi.org/10.1039/C2LC40690J>
- Chami Khazraji A, Robert S (2013) Interaction effects between cellulose and water in nanocrystalline and amorphous regions: a novel approach using molecular modeling. *J. Nanomater.* <https://www.hindawi.com/journals/jnm/2013/409676/>.
- Chapman R, Lin Y, Burnapp M, Bentham A, Hillier D, Zabron A, Khan S, Tyreman M, Stevens MM (2015) Multivalent nanoparticle networks enable point-of-care detection of human phospholipase-A2 in serum. *ACS Nano* 9:2565–2573. <https://doi.org/10.1021/nm5057595>
- Chen X, Leng Y, Hao L, Duan H, Yuan J, Zhang W, Huang X, Xiong Y (2020) Self-assembled colloidal gold superparticles to enhance the sensitivity of lateral flow immunoassays with sandwich format. *Theranostics* 10:3737–3748. <https://doi.org/10.7150/thno.42364>
- Choi DH, Lee SK, Oh YK, Bae BW, Lee SD, Kim S, Shin Y-B, Kim M-G (2010) A dual gold nanoparticle conjugate-based lateral flow assay (LFA) method for the analysis of troponin I. *Biosens Bioelectron* 25:1999–2002. <https://doi.org/10.1016/j.bios.2010.01.019>
- Choi JR, Liu Z, Hu J, Tang R, Gong Y, Feng S, Ren H, Wen T, Yang H, Qu Z, Pingguan-Murphy B, Xu F (2016) Polydimethylsiloxane-paper hybrid lateral flow assay for highly sensitive point-of-care nucleic acid testing. *Anal Chem* 88:6254–6264. <https://doi.org/10.1021/acs.analchem.6b00195>
- Dincer C, Bruch R, Kling A, Dittrich PS, Urban GA (2017) Multiplexed point-of-care testing – xPOCT. *Trends Biotechnol* 35:728–742. <https://doi.org/10.1016/j.tibtech.2017.03.013>
- Drain PK, Hyle EP, Noubary F, Freedberg KA, Wilson D, Bishai WR, Rodriguez W, Bassett IV (2014) Diagnostic point-of-care tests in resource-limited settings. *Lancet Infect Dis* 14:239–249. [https://doi.org/10.1016/S1473-3099\(13\)70250-0](https://doi.org/10.1016/S1473-3099(13)70250-0)
- Fatehi P, Xiao H, van de Ven TGM (2011) Quantitative analysis of cationic poly(vinyl alcohol) diffusion into the hairy structure of cellulose fiber pores: charge density effect. *Langmuir* 27:13489–13496. <https://doi.org/10.1021/la203364x>
- Fu E, Lutz B, Kauffman P, Yager P (2010) Controlled reagent transport in disposable 2D paper networks. *Lab Chip* 10:918–920. <https://doi.org/10.1039/B919614E>
- Gong X, Cai J, Zhang B, Zhao Q, Piao J, Peng W, Gao W, Zhou D, Zhao M, Chang J (2017) A review of fluorescent signal-based lateral flow immunochromatographic strips. *J Mater Chem B* 5:5079–5091. <https://doi.org/10.1039/C7TB01049D>
- Han G-R, Koo HJ, Ki H, Kim M-G (2020) Paper/soluble polymer hybrid-based lateral flow biosensing platform for high-performance point-of-care testing. *ACS Appl Mater Interfaces* 12:34564–34575. <https://doi.org/10.1021/acsami.0c07893>
- He P, Wu J, Pan X, Chen L, Liu K, Gao H, Wu H, Cao S, Huang L, Ni Y (2020) Anti-freezing and moisturizing conductive hydrogels for strain sensing and moist-electric generation applications. *J Mater Chem A* 8:3109–3118. <https://doi.org/10.1039/C9TA12940E>
- He W, You M, Li Z, Cao L, Xu F, Li F, Li A (2021) Upconversion nanoparticles-based lateral flow immunoassay for point-of-care diagnosis of periodontitis. *Sens Actuators B Chem* 334:129673. <https://doi.org/10.1016/j.snb.2021.129673>
- Houghtaling J, Liang T, Thiessen G, Fu E (2013) Dissolvable bridges for manipulating fluid volumes in paper networks. *Anal Chem* 85:11201–11204. <https://doi.org/10.1021/ac4022677>
- Hu K, He P, Zhao Z, Huang L, Liu K, Lin S, Zhang M, Wu H, Chen L, Ni Y (2021) Nature-inspired self-powered cellulose nanofibrils hydrogels with high sensitivity and mechanical adaptability. *Carbohydr Polym* 264:117995. <https://doi.org/10.1016/j.carbpol.2021.117995>
- Huang X, Aguilar ZP, Xu H, Lai W, Xiong Y (2016) Membrane-based lateral flow immunochromatographic strip with nanoparticles as reporters for detection: a review. *Biosens Bioelectron* 75:166–180. <https://doi.org/10.1016/j.bios.2015.08.032>
- Huang X, Zhou Y, Ding L, Yu G, Leng Y, Lai W, Xiong Y, Chen X (2019) Supramolecular recognition-mediated

- layer-by-layer self-assembled gold nanoparticles for customized sensitivity in paper-based strip nanobiosensors. *Small* 15:1903861. <https://doi.org/10.1002/sml.201903861>
- Hwang J, Lee S, Choo J (2016) Application of a SERS-based lateral flow immunoassay strip for the rapid and sensitive detection of staphylococcal enterotoxin B. *Nanoscale* 8:11418–11425. <https://doi.org/10.1039/C5NR07243C>
- Jani IV, Peter TF (2013) how point-of-care testing could drive innovation in global health. *New Engl J Med* 368(24):2319. <https://doi.org/10.1056/NEJMs1214197>
- Khan IH, Sayeed MA, Sultana N, Islam K, Amin J, Faruk MO, Khan U, Khanam F, Ryan ET, Qadri F (2016) Development of a simple, peripheral-blood-based lateral-flow dipstick assay for accurate detection of patients with enteric fever. *Clin Vaccine Immunol CVI* 23:403–409. <https://doi.org/10.1128/CVI.00690-15>
- Li Z, You M, Bai Y, Gong Y, Xu F (2020) Equipment-Free Quantitative Readout in Paper-Based Point-of-Care Testing. *Small Methods* 4:1900459. <https://doi.org/10.1002/smt.201900459>
- Lutz B, Liang T, Fu E, Ramachandran S, Kauffman P, Yager P (2013) Dissolvable fluidic time delays for programming multi-step assays in instrument-free paper diagnostics. *Lab Chip* 13:2840–2847. <https://doi.org/10.1039/C3LC50178G>
- Posthuma-Trumpie GA, Korf J, van Amerongen A (2009) Lateral flow (immuno)assay: its strengths, weaknesses, opportunities and threats. *A Lit Surv Anal Bioanal Chem* 393:569–582. <https://doi.org/10.1007/s00216-008-2287-2>
- Rivas L, Medina-Sánchez M, de la Escosura-Muñoz A, Merkoçi A (2014) Improving sensitivity of gold nanoparticle-based lateral flow assays by using wax-printed pillars as delay barriers of microfluidics. *Lab Chip* 14:4406–4414. <https://doi.org/10.1039/C4LC00972J>
- Sajid M, Kawde A-N, Daud M (2015) Designs, formats and applications of lateral flow assay: a literature review. *J Saudi Chem Soc* 19:689–705. <https://doi.org/10.1016/j.jscs.2014.09.001>
- Sena-Torralba A, Ngo DB, Parolo C, Hu L, Álvarez-Diduk R, Bergua JF, Rosati G, Surareungchai W, Merkoçi A (2020) Lateral flow assay modified with time-delay wax barriers as a sensitivity and signal enhancement strategy. *Biosens Bioelectron* 168:112559. <https://doi.org/10.1016/j.bios.2020.112559>
- Tang R, Yang H, Gong Y, Liu Z, Li X, Wen T, Qu Z, Zhang S, Mei Q, Xu F (2017) Improved analytical sensitivity of lateral flow assay using sponge for HBV nucleic acid detection. *Sci Rep* 7:1360. <https://doi.org/10.1038/s41598-017-01558-x>
- Tang RH, Liu LN, Zhang SF, Li A, Li Z (2019) Modification of a nitrocellulose membrane with cellulose nanofibers for enhanced sensitivity of lateral flow assays: application to the determination of *Staphylococcus aureus*. *Microchim Acta* 186:831. <https://doi.org/10.1007/s00604-019-3970-z>
- Tang RH, Li M, Liu LN, Zhang SF, Alam N, You M, Ni YH, Li ZD (2020) Chitosan-modified nitrocellulose membrane for paper-based point-of-care testing. *Cellulose* 27:3835–3846. <https://doi.org/10.1007/s10570-020-03031-x>
- Tang R, Alam N, Li M, Xie M, Ni Y (2021) Dissolvable sugar barriers to enhance the sensitivity of nitrocellulose membrane lateral flow assay for COVID-19 nucleic acid. *Carbohydr Polym* 268:118259. <https://doi.org/10.1016/j.carbpol.2021.118259>
- Vashist SK, Lippa PB, Yeo LY, Ozcan A, Luong JHT (2015) Emerging technologies for next-generation point-of-care testing. *Trends Biotechnol* 33:692–705. <https://doi.org/10.1016/j.tibtech.2015.09.001>
- Wood CS, Thomas MR, Budd J, Mashamba-Thompson TP, Herbst K, Pillay D, Peeling RW, Johnson AM, McKendry RA, Stevens MM (2019) Taking connected mobile-health diagnostics of infectious diseases to the field. *Nature* 566:467–474. <https://doi.org/10.1038/s41586-019-0956-2>
- Yuan Z, Lin H, Qian X, Shen J (2019) Converting a dilute slurry of hollow tube-like papermaking fibers into phase-reversible, self-healable, and stretchable hydrogels. *J Bioreour Bioprod* 4:214–221. <https://doi.org/10.12162/jbb.v4i4.011>
- Zhao S, Wang S, Zhang S, Liu J, Dong Y (2018) State of the art: Lateral flow assay (LFA) biosensor for on-site rapid detection. *Chin Chem Lett* 29:1567–1577. <https://doi.org/10.1016/j.ccl.2017.12.008>

Publisher's Note Springer Nature remains neutral with regard to jurisdictional claims in published maps and institutional affiliations.